PERGAMON

Computers & Geosciences 27 (2001) 203–213

COMPUTERS & GEOSCIENCES

Reflectance processing of remote sensing spectroradiometer data☆

Derek R. Peddle [a,*,1], H. Peter White[b,2], Raymond J. Soffer[c,3], John R. Miller[b], Ellsworth F. LeDrew[d]

[a] *Department of Geography, University of Lethbridge, Lethbridge, Alberta, Canada T1K 3M4*
[b] *Department of Physics and Astronomy, CRESTech, York University, North York, Ont., Canada M3J 1P3*
[c] *Instrument Services Laboratory, CRESTech, York University, North York, Ont., Canada M3J 1P3*
[d] *Department of Geography, University of Waterloo, Waterloo, Ont., Canada N2L 3G1*

Received 18 September 1998; received in revised form 4 May 2000; accepted 4 May 2000

Abstract

Spectral reflectance is the ratio of incident-to-reflected radiant flux measured from an object or area over specified wavelengths. Unlike radiance and irradiance values, reflectance is an inherent property of an object and is independent of time, location, illumination intensity, atmospheric conditions and weather. Although reflectance is a key unit of measure in remote sensing, it is not measured directly and instead must be derived. Accordingly, the conversion of field and laboratory measurements of spectral radiance into reflectance values is a frequent requirement with ground data in support of airborne and satellite remote sensing applications in the environmental and earth sciences. In this paper, laboratory and computer methods for processing field spectroradiometer measurements of spectral radiance into calibrated absolute reflectance values are described. Target radiance measures are obtained under direct and diffuse illumination using a portable field spectroradiometer, with irradiance spectra captured by near simultaneous acquisition of reflected radiation from a reference panel. The approach for converting raw target and panel radiance spectra to calibrated reflectance involves five major processing stages: (i) panel calibration, (ii) solar zenith angle computations, (iii) spectral and angular interpolation, (iv) computation of reflectance, and (v) automated batch mode execution of stages (ii)–(iv) for processing large data volumes. Equipment, methods, and computer programs for achieving these stages are described. Example forestry ground spectra acquired in the Boreal Ecosystem Atmosphere Study (BOREAS) are presented to illustrate raw field measurements and final reflectance products. These methods would also be useful in other applications such as agriculture, water resources, oceanic studies, rangeland management, and geological exploration and mineral identification.

Keywords: Remote sensing; Reflectance; Spectroradiometer; BOREAS; Calibration; Radiance

1. Introduction

Field measurements of surface reflectance are used in a number of remote sensing analytical approaches such as vegetation canopy reflectance modelling (Strahler and Jupp, 1990; Li and Strahler, 1992; Rosema et al., 1992), spectral mixture analysis (Adams et al., 1993), satellite and airborne image classification and predictive modelling (Franklin, 1995), and surface validation in terrestrial ecology, ecosystem process and energy exchange

☆Code available at http://www.iamg.org/CGEditor/index.htm.

*Corresponding author.Tel.: 1-403-329-2524; fax: 1-403-329-2016.

E-mail address: derek.peddle@uleth.ca (D.R. Peddle).

[1] http://home.uleth.ca/geo/derekp.htm.

[2] Current address: Canada Centre for Remote Sensing, Natural Resources Canada, Ottawa, Ont., Canada K1A 0Y7.

[3] Current address: Routes AstroEngineering, Kanata, Ont., Canada K2K 2B1.

0098-3004/01/$ - see front matter
PII: S0098-3004(00)00096-0

models (Sellers and Schimel, 1993; Blackburn and Milton, 1995). These spectra are also useful in atmospheric correction, validation and reflectance calibration of remote sensing imagery and for sensor calibration and inter-comparison based on ground targets of known spectral properties (O'Neil et al., 1997; Milton and Goetz, 1997; Middleton et al., 1997; Gray et al., 1997). Spectral data are typically obtained for small areas at ground level or from tower platforms in a variety of configurations using portable field spectroradiometers (Deering, 1989; Milton et al., 1995) which provide highly detailed spectral information of known targets identified in the field (Teillet, 1995). These instruments measure the amount of energy reflected from a ground area or object of interest over different wavelengths (Milton, 1987), and these measurements can be converted to spectral radiance values if appropriate equipment calibration factors exist. The magnitude of spectral radiance depends on the amount of incoming solar radiation (spectral irradiance) reaching the target, and this can vary significantly according to date and time of day (solar zenith angle, path length), atmospheric conditions and weather, topography and local orientation of the surface, and intervening features which may further alter or attenuate incoming radiation (e.g. forest canopies, shadowing). The ratio of incident-to-reflected radiant flux over specified wavelengths is termed spectral reflectance, which, as pointed out by Curran (1985), is a term often used mistakenly in the literature instead of radiance. Reflectance is an inherent property of an object which, unlike radiance and irradiance values, is independent of the intensity and nature of illumination. As a result, reflectance is generally the standard unit in remote sensing when using information from different sensors, times, or locations, or when comparing spectral measurements against known reflectance properties of objects (e.g. mineral identification from spectral libraries, geologic exploration). For a given spectral measurement, the angular measure of radiance is converted to a bidirectional reflectance factor (BRF); that is, the spectral radiance measured at a specified view angle to the object of interest ratioed by the irradiance at a given angle of incidence illumination.

In this paper, we describe computer analysis methods developed for processing raw field spectra to calibrated reflectance measurements. This involves (i) laboratory calibration of reference panels; (ii) computing the solar zenith angle (SZA) for a given field measurement based on date, time, and global position; (iii) spectral and angular interpolation of calibration coefficients and derivation of the appropriate coefficient for the computed SZA; (iv) computation of reflectance, and (v) computer software to coordinate these stages into an integrated and automated environment for reflectance processing of large volumes of field data. Equipment, methods, and computer programs for achieving these stages are presented, and illustrated with an example of raw ground spectra acquired in the field using a portable field spectroradiometer (ASD, 1993) and the resulting reflectance spectra derived from the processing described herein. Forestry examples from the Boreal Ecosystem Atmosphere Study (BOREAS) are presented to illustrate these ideas. We note that these reflectance processing methods have also been used in other applications involving agriculture, mountain terrain analysis, polar sea ice, and tropical ocean coral reefs (Misurak et al., 1993; Peddle et al., 1995, 1999a; Johnson et al., 1999; Peddle and Johnson, 2000) and would be suitable for a wide range of other applications such as geology, water resources, ecology, and others.

2. Reference panels and calibration

2.1. Reference panels

Radiance is normally obtained in the field by nadir measurement of specific ground targets, with incoming solar irradiance spectra typically acquired from coincident measurement of reflected energy flux from reference panels with known spectral and angular scattering properties. Several types of reference panels and materials are available. Examples include barium sulphate ($BaSO_4$) (Jackson et al., 1992), pressed polytetrafluoroethylene (PTFE) (Weidner and Hsia, 1981) which is available commercially as Spectralon (Labsphere, 1998), as well as neutral test cards (Milton, 1989) manufactured as standards for use in colour photography. PTFE offers nearly ideal Lambertian properties and high reflectance values (95–99% for white surfaces) over a broad spectral range (350–2500 nm). The primary disadvantage of PTFE is the higher cost, with secondary factors including the need to maintain a clean surface and to avoid damage or loss. Neutral test cards such as Kodak Grey Cards (Eastman Kodak, 1983) have the advantage of significantly lower cost, to the point that they may be replaced frequently in the field, while providing reasonably consistent absolute reflectance values in the range 80–90% (white side of card) between 500 and 1000 nm (Palmer, 1982; Philipson et al., 1989; Milton, 1989). In this work, we have developed calibration and processing methods for use with Kodak Grey Cards (KGC), however, we note that some or all of the processing steps would be applicable to other reference panels and materials.

2.2. Panel calibration

It is essential that reference panel measurements be calibrated, since panels and KGCs do not reflect all of the incident radiation, and further, their reflectance can be highly dependent on illumination angle (solar zenith

angle). In some cases, panel-specific calibration coefficients can be purchased for certain types of reference panels at additional cost, or general calibrations can be used in which stated calibration variations must be tolerated (Milton, 1989). In the case of Kodak Grey Cards, neither of these calibration options are available. Accordingly, a laboratory panel calibration facility was developed at the Instrument Services Laboratory (ISL) for characterising the spectral properties of Kodak Grey Cards in terms of bidirectional reflectance factors (BRF). A full description of this facility is contained in Soffer et al. (1995), and is only summarised here briefly.

The ISL calibration facility used an Ocean Optics ST1000 spectroradiometer which has 1024 channels between 360 and 860 nm. The spectroradiometer was connected to a detector head mounted on a precision controlled rotational stage to permit spectral acquisition over a range of user-specified view angles. The panel was secured to a second rotational stage for setting the illumination angle. The small size of the detector head and the positional flexibility of the system permitted reliable measurement in the case of near-coincident view and illumination angles. Using nadir illumination (to minimise experimental error), a series of KGCs were characterised at view angles between 15 and 80°, at 5° increments. Then, according to the Helmholz reciprocity principle (Hsia and Weidner, 1981), which states that a BRF at view angle δ and nadir illumination is equivalent to that obtained at nadir view angle and illumination angle δ, we interpreted those view angles as solar zenith angles (SZA) for the purpose of deriving panel calibrations over the wide range of SZAs encountered in the field. Validation of the system was accomplished through comparisons of facility results for a 99% PTFE (Spectralon) Panel with published BRFs of that material, and with facility results from BOREAS instrument calibrations at the University of Nebraska, USA.

The BRFs of the white side of the rectangular KGCs differed significantly between the two orthogonal panel orientations, suggesting that this variable should be noted in the field and accounted for in the laboratory. In our field work, the longer axis of the KGC was always aligned with the solar plane, allowing us to use the BRFs obtained from the view angle plane oriented 90° to the KGC narrow dimension for calibration. Once these panel orientation effects were separated, the combined variability of BRFs among five KGCs cards used in the field was assessed together with a new, clean KGC in terms of spatial differences within each card, differences between cards, and experimental error. The variability was very low, which permitted one BRF to be generated for use with all 6 cards.

An inter-sensor comparison was also performed between the Ocean Optics spectroradiometer used in the laboratory, and the ASD spectroradiometer used in the field. The size of the ASD spectroradiometer FOV barrel made it impractical to obtain a full range of angular measurements in the laboratory necessary for panel BRF characterisation over a full range of SZAs that may be encountered in the field. Instead, several ASD spectra of KGCs were collected in the panel calibration facility at nadir illumination and view angles between 50 and 60°, for comparison with similarly acquired spectra using the methods described here. The results were consistent between the two spectroradiometer instruments tested. The final output of the panel calibration process was an Excel spreadsheet (Microsoft, 1997) containing target BRFs between 350 and 850 nm at 14 view angles (SZAs) for 11 spectral wavebands at 50 nm intervals, plus an additional 4 bands at wavelengths used with a modular multiband radiometer (MMR) instrument. Degrading the spectral resolution to 50 nm made the panel calibration files more manageable given the large volume of field data being processed. This was done after results from high-order interpolations of the 15 wavebands (discussed later) showed a very high correspondence with the high spectral resolution raw spectra.

3. Solar zenith angle computations

Knowledge of the SZA for a given field measurement is critical as a result of the reflectance anisotropy for nadir observations of coniferous forest canopies (Syrén, 1994) and other surfaces (Rollin et al., 2000). However, since it can be difficult to determine SZA with any degree of confidence while in the field without dedicated equipment for that purpose, an alternative post-processing method was required to allow accurate specification of SZA for the reflectance processing software.

To determine the solar zenith and azimuth angles accurately for a given spectral observation, only the date and time of measurement, and the latitude and longitude are required. The date and local time were stored automatically in the header of each ASD spectra file, with the exact latitude and longitude of the field sites obtained from global positioning systems (GPS) or maps. Determining the solar position from time and location is a standard computation in astronomical and planetary studies (Duffett-Smith, 1990; Bishop, 1994). This was encoded in an Excel spreadsheet, which is summarised here to be readily accessible to the remote sensing and environmental earth sciences communities in a concise form, together with equations provided in Appendix A.

First, the date and time must be converted such that it is not dependent on the specific location or on calendar variations. This is achieved by converting the date to Julian Days (JD, the number of days since 1 January 4713 BC) and converting time to fraction of a day (TM).

The position of the Sun for that day is then determined, using Eqs. (A.1)–(A.4) in Appendix A, in terms of the mean solar longitude (L_Θ, the location of the Sun if the Earth had a perfectly circular orbit), the mean solar anomaly (g, the angular distance of the Sun from perigee due to the Earth's elliptical orbit), and the solar ecliptic longitude (L_e, the true longitude of the Sun along the ecliptic line). With the location of the Sun known along the ecliptic, the right ascension and declination of the Sun for the given time (RA_Θ, DEC_Θ) can then be calculated in terms of the obliquity of the ecliptic (oe), using Eqs. (A.5)–(A.7). Once these have been determined, the right ascension and declination of the zenith point (RA_z, DEC_z) of the observation are the final terms required for computing solar position. DEC_z is the site latitude (Eq. (A.8)). The term RA_z is defined as the local mean sidereal time (LMST) of the observation, computed as a longitudinal offset from the greenwich mean sidereal time (GMST), using Eqs. (A.9)–(A.12). With the exact locations of the Sun and the zenith known, the solar zenith angle (SZA, or Z_Θ, the standard angular distance of the Sun from zenith) and solar azimuth angle (Az_Θ, number of degrees the Sun is east of north) are determined using Eqs. (A.13)–(A.14). The SZA computed for a given field measurement represents one of the initial inputs to the calculation of reflectance, presented next.

4. Spectral and angular interpolation

The result of the panel calibration is a matrix of BRFs for the KGCs at 50 nm wavelength intervals for 15 view angles. However, panel calibration data were required for the specific SZA encountered in the field (computed as above for each field measure), and further, these data must be determined at high spectral resolutions matching that of the field spectroradiometer. Therefore, to achieve this level of precision, spectral and angular interpolations were applied to the original panel calibration results using an Excel spreadsheet (Microsoft, 1997) shown in Fig. 1. Although much of the Excel code and formulations are hidden or contained elsewhere in the spreadsheet, a number of important functions are illustrated. The angular interpolation is performed first. For each centre wavelength (column B in Fig. 1), an equation describing the BRFs over the 15 angular measures is determined using a fourth-order polynomial fit applied to the panel calibration data (read from a separate worksheet, not shown), as this provided the best fit for all reference panels over a variety of angles. Using these equations, target BRFs (column F) are calculated for each centre wavelength for the input SZA (obtained by referencing the linked SZA worksheet which computes the solar position for the field spectral measurement). Next, the spectral interpolation is performed over these target BRFs for the specified SZA. This is done by fitting an equation to the points described by the target BRFs at MMR and standard wavelengths (STD), again, using a fourth-order polynomial. The coefficients of that equation, their standard errors, and the r^2 value for the equation are shown in the box above the chart in Fig. 1. In the example, the r^2 value was very high (>0.99), which is a typical result as the fourth-order polynomials provided highly accurate spectral and angular interpolations. This was expected, given the stable spectral response observed for a variety of panels over a range of view angles, and allowed the panel calibration process to be simplified in terms of the number of spectra and bandwidths required to produce optimal spectral characterisations in the laboratory.

The results of applying these equations back to the original centre wavelengths are displayed in Fig. 1 (top portion of column G), with the associated standard error for each estimate shown (column H). In this example, panel calibration data for the grey side of a KGC panel are shown (Fig. 1). The chart includes the full equation, its r^2 value, and a plot of the curve for the equation fit to the target BRF points, displayed as diamonds along the curve. These equations were then applied to compute panel calibration BRFs at each wavelength band of the field spectroradiometer which, for the ASD instrument, was at 1.423 nm intervals. These results, shown in the bottom right of Fig. 1, represent the output from the spectral and angular interpolation of the panel calibration data used in computing reflectance.

5. Automated reflectance processing and an example

5.1. Reflectance processing software

Software to compute reflectance from field spectral measurements of radiance and irradiance are sometimes available from manufacturers or spectral laboratories (e.g. PIMAVIEW). In this research, an Excel macro program was written to control batch mode execution of reflectance processing involving large volumes of field spectroradiometer data. The process involved three linked Excel spreadsheets, each with different functions, together with input spectra files and a series of batch command modules. The spreadsheets contain: (i) the laboratory panel calibration BRFs of the KGCs, as discussed earlier; (ii) the solar zenith angle computations; and, (iii) the angular and spectral interpolation routines. The external files, which are read into the macro program for input to the spreadsheets, included the target and panel spectra files collected in the field [converted from binary to ASCII format using the ASD (1993) Portspec command], each of which contained

Input Solar Zenith Angle :	51.55		Panel: KGC - Gray Side				
A	B	C	D	E	F	G	H
Band Designation	Center Wavelength (nm)	Start Wavelength (nm)	End Wavelength (nm)		**Target BRF**	**4th Order Fit BRF**	**St. Error (percent)**
MMR1-485	484.8400	449.5900	520.0900		0.17221	0.17481	1.51%
MMR2-560	560.5100	520.0900	600.9300		0.16977	0.16970	-0.04%
MMR3-660	660.0750	629.2900	690.8600		0.17285	0.17055	-1.33%
MMR4-809	809.2100	760.2300	858.1900		0.21398	0.21599	0.94%
STD01-358	358.1450	341.3500	374.9400		0.08093	0.08246	1.89%
STD02-400	400.3000	374.9400	425.6600		0.14194	0.13947	-1.74%
STD03-450	450.5550	425.6600	475.4500		0.17194	0.16930	-1.54%
STD04-500	499.8750	475.4500	524.3000		0.17250	0.17496	1.43%
STD05-550	549.2900	524.3000	574.2800		0.17074	0.17089	0.09%
STD06-600	599.7700	574.2800	625.2600		0.16685	0.16684	-0.01%
STD07-650	650.2000	625.2600	675.1400		0.17133	0.16911	-1.30%
STD08-700	700.4850	675.1400	725.8300		0.17624	0.17976	2.00%
STD09-750	750.5850	725.8300	775.3400		0.19814	0.19666	-0.75%
STD10-800	800.4100	775.3400	825.4800		0.21344	0.21366	0.10%
STD11-850	841.8350	825.4800	858.1900		0.22215	0.22086	-0.58%
4th Order Equation of Fit:		y=Ax^4+Bx^3+Cx^2+Dx+E					
		Coefficient	St. Error			ASD Wavelength	4th Order Fit BRF
	A=	-2.6908E-11	2.05627E-12			400.01	0.1454
	B=	6.9999E-08	4.92391E-09			401.42	0.1462
	C=	-6.6562E-05	4.3178E-06			:	:
	D=	0.027493102	0.001640413			:	:
	E=	-3.999268049	0.227450551			:	:
	R2=	0.996287914				:	:
						:	:
						:	:
						:	:
						:	:
						:	:
						:	:
						:	:
						:	:
						:	:
						:	:
						:	:
						:	:
						:	:
						:	:
						:	:
						848.61	0.2298
						850.02	0.2314

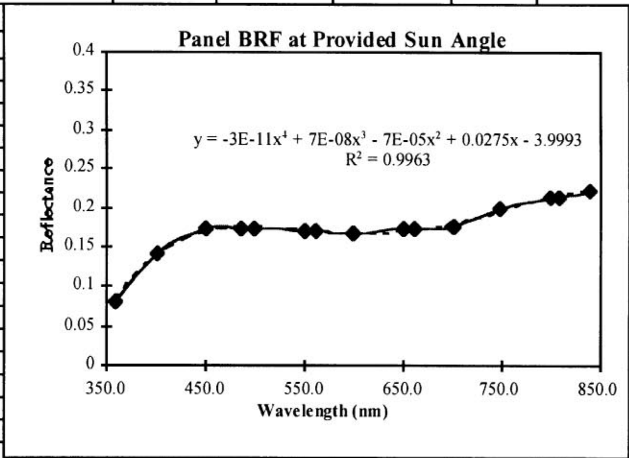

Fig. 1. Excel spreadsheet for spectral and angular interpolation of panel calibration BRFs.

important header information. The only requirement of the user is to create a batch file which specifies the target and panel file names, the output reflectance file name, the latitude and longitude of the field site, and several comment fields of text describing the spectral acquisition (e.g. target species, sampling design, site description, illumination conditions, KGC panel information, spectrum characteristics, etc.). These batch files can be created using any standard word processing software or system editor.

The first task the macro program performs is to prompt the user for the name of the batch control file using an interactive dialogue box — this is the only user intervention required when running the software. After the file name has been supplied, the macro runs in stand-alone, unattended batch mode. During program execution, it first reads the latitude and longitude of the field site from the batch file, together with the additional site and data descriptors, and one set of target, panel, and output reflectance file names. The raw spectra digital numbers are read from the target and panel files (see Fig. 2), and placed in a new output file to which reflectance values are later written (Table 1). Using a series of parsing functions, the acquisition date and time for the target spectrum are extracted from the ASD target file header and input to the SZA worksheet together with the site latitude and longitude. The SZA worksheet is then recalculated to compute the SZA for the time of target spectra acquisition. The macro reads the output SZA, and writes it to the spectral and angular interpolation worksheet (Fig. 1), from which the panel calibration fourth-order polynomial BRFs over the field spectroradiometer wavelengths are computed. The macro then extracts these panel calibrations, and places them in the reflectance file. Spectral reflectance for a given SZA (σ) and at nadir view angle (θ) is then computed over the full wavelength range at the spectral resolution of the field spectroradiometer as:

$$\text{Reflectance}_{(\sigma,\theta)} = \frac{\text{target radiance}}{\text{panel radiance}} \times \text{panel calibration BRF}. \quad (1)$$

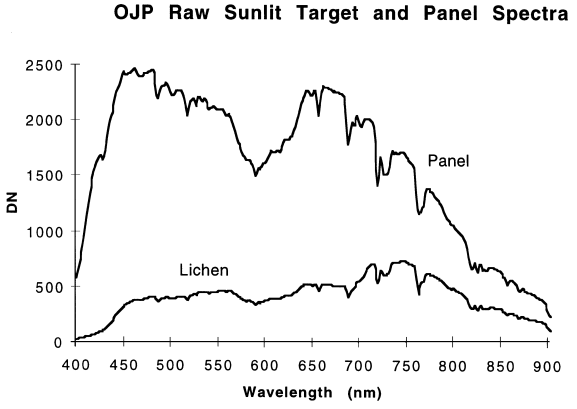

Fig. 2. Raw spectral digital number (DN) field measurements of sunlit lichen target and Kodak Grey Card (KGC) white reference panel used in computation of reflectance. Spectra shown from BOREAS SSA OJP during 1994 IFC-3.

Once reflectance has been computed, the macro invokes a number of procedures to compile information describing the various parameters associated with the data acquisition (mentioned above), which were obtained from the set of worksheets and external files. These are synthesised and formatted into a header template and written to the reflectance output file. Once this has been done, the relevant files are closed, and the entire procedure is repeated using a looping function to process the next set of panel and target spectra, as listed in the batch file. The output reflectance files are produced in ASCII format and are suitable for input to graphics programs, statistical software packages or image processing routines for further analysis. A portion of an example output reflectance file is shown in Table 1. Example plots of reflectance spectra curves processed using these methods are presented in the next section. The full Excel macro and spreadsheets, including a set of KGC panel calibrations (white and grey sides) and a test file are contained on the public domain *Computers & Geosciences* ftp site (ftp.iamg.org).

5.2. Example reflectance spectra

A large number of field spectroradiometer measurements were acquired during 5 field campaigns from January to September 1994 as part of the Boreal Ecosystem Atmosphere Study (BOREAS), a large international global change research project in the Canadian boreal forest (Sellers et al., 1995). As one of 80 scientific projects in BOREAS, our Remote Sensing Science project (RSS-19) measured and computed understorey reflectance spectra as a contribution to the BOREAS information system, and for use in our research (e.g. Miller et al., 1997; Peddle et al., 1997). To illustrate the methods and programs presented in this paper, in this section we present and describe briefly a set of raw field measurements (Fig. 2) and the resulting final spectra (Fig. 3) produced by reflectance processing.

The spectra shown in Figs. 2 and 3 were acquired on 13 September 1994 during the late summer intensive field campaign (IFC-3) at the Old Jack Pine site in the BOREAS southern study area (SSA-OJP) in Saskatchewan Canada. In Fig. 2, the target and reference panel measurements are shown from raw spectral data collected in the field. These field spectra form the required spectral measurements necessary to compute reflectance. In this example, the target viewed under sunlit illumination was lichen (*Cladina mitis*, see Halliwell and Apps, 1996), which is the dominant ground cover species within the Old Jack Pine forest. Spectral measurements of ground cover vegetation are of interest in remote sensing studies since, when viewed from a nadir mounted platform, the understorey and background vegetation beneath a forested canopy can contribute a significant component of the overall

Table 1
Example output reflectance file from computer macro program. Each file contains header information describing field spectroradiometer and data collection parameters, as well as final processed reflectance values (full table not shown)

BOREAS data — reflectance spectra	
BOREAS project:	RSS-19
Field campaign:	IFC-3
Field instrument:	ASD spectroradiometer
Panel calibration:	Kodak Grey Card (White Side)
Reflectance data specifications	
Spectral range:	400–900 nm
Wavelength step:	1.4230 nm
Spectrum description:	Average of 10 spectra; 10° FOV
Location:	SSA OJP Tower (G2L3 T)
Latitude (+°N; −°S):	53.914
Longitude (+°E; −°W):	−104.6925
Date:	9/13/94
Time (Local):	13:50:37 (1:50 PM)
Time (GMT):	19:50:37
Solar zenith angle (°):	51.55
Solar azimuth (°):	197.95
Target description:	LICHEN
Illumination:	SUNLIT
Comments:	PFL / CLEAR SKIES
Reflectance data	
Wavelength (start)	Reflectance
400.00	0.041
401.41	0.039
402.83	0.041
404.26	0.041
::	::
::	::
896.61	0.311
898.03	0.306
899.45	0.305
900.88	0.301

reflected energy received at an airborne or satellite sensor. As a result, these background spectra are often required inputs to canopy radiation models (e.g. Li and Strahler, 1992; Rosema et al., 1992; Hall et al., 1997; Peddle et al., 1997) and spectral mixture analysis algorithms (e.g. Roberts et al., 1993; Nelson et al., 1994; Hall et al., 1995; Peddle et al., 1999b). Spectra such as these are also useful for detailed analyses in their own right (Franklin et al., 1991; Hanan et al., 1993; Goward et al., 1994; Peddle, 1998).

The plot in Fig. 2 shows the raw spectral digital numbers (DN) for the target sunlit background lichen and the corresponding KGC panel reference spectra for that time and location, taken several seconds after the target spectra. In this example, the white side of the KGC reference panel was used. As can be seen in the plot, the reference panel spectral values are greater than the target spectral values, as expected. In Fig. 2, significant changes in the magnitude of difference between target and panel measurements are seen in the region bounded by ~550–760 nm, in which vegetation spectral response features such as the green peak and red edge occur.

In Fig. 3, the resulting reflectance spectrum for the background sunlit lichen is shown. At each wavelength interval, reflectance was computed as a function of the target and reference panel measurements (Fig. 2), using calibration BRFs from the white side of a KFC panel using the methods described earlier (Eq. (1)). This type of lichen has a brighter appearance in the field, which is manifested as higher overall reflectance values throughout the visible portion of the electromagnetic spectrum compared to other background species. Reflectance throughout most of the visible portion of the spectrum ranged to about 0.20 (or 20%), with a slight green peak noticeable near 550 nm where plant pigments are responsible for the scattering of light which causes vegetation to appear green. The red-edge is evident from 680 to 760 nm, although the difference in magnitude of reflectance in the red and NIR is less pronounced

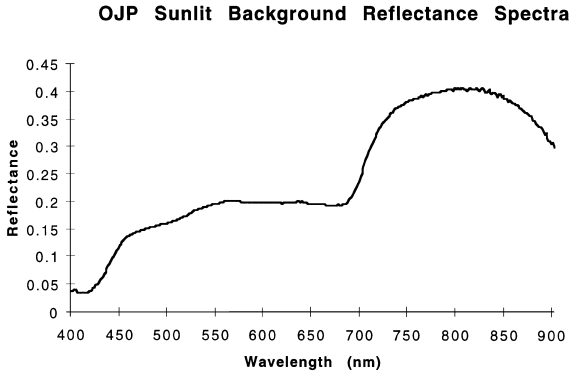

Fig. 3. Sunlit background reflectance spectra of lichen derived using field spectroradiometer measurements from Old Jack Pine forest stand. Original field and panel spectra shown in Fig. 2.

compared to other forest vegetation, in part due to the higher reflectance in the adjacent green portion of the spectrum. Maximum reflectance values range to 0.40 in the NIR region. These spectra have been used in a variety of ecological and biophysical applications, including input to canopy reflectance models, spectral mixture analyses, vegetation index studies, and temporal analyses of the growth and seasonal evolution of forest vegetation species (Miller et al., 1997; Peddle et al., 1997; Hall et al., 1997). A full account of the understorey vegetation field spectra collected as part of the BOREAS project, as well as additional examples and applications of these spectra have been published previously by Miller et al. (1997), and are not repeated here.

6. Conclusion

The processing of raw field spectra into calibrated reflectance forms an important part of most remote sensing projects which use ground spectroradiometer data in support of airborne or satellite image analysis. For example, reflectance values processed from field spectroradiometer data are frequently used in forestry and agricultural studies to provide key information on vegetation monitoring and ecological properties, or in geology to aid in surface material identification and mineral exploration. Field or laboratory reflectance data can also provide a sole source of information (independent of remote sensing imagery), such as with surface target identification using pattern search and matching techniques with known reflectance curves from established spectral libraries.

In this paper, a flexible and automated approach for producing spectral reflectance values from field spectroradiometer data has been presented. The approach is flexible in that panel calibration data for any solar zenith angle can be derived based on procedures for spectral and angular interpolation of panel measurements obtained over a range of view angles in a laboratory setting. In this work, laboratory calibration spectra were obtained for Kodak neutral test cards used in the field, which have been shown to be good reference standards at reasonable cost (Milton, 1989). These calibration spectra have also been useful for subsequent applications using different KGC products. An extensive macro program controls batch processing of large volumes of spectral data in an automated environment — the user need only generate a batch file specifying the location of spectral measurements and file names for processing. The approach permits high-quality reflectance values to be obtained from the data collected in the field.

In this work, we have described laboratory and computer processing methods for specific types of spectroradiometers and reference panels, with software code placed in the public domain. This approach has recently been modified at the University of Lethbridge for use with an ASD FR spectroradiometer with a spectral range 350–2500 nm (ASD, 1998) and simplified for use with a calibrated PTFE (Spectralon) panel. We note further that these general methods and approaches may be suitable for other equipment and materials, and in other remote sensing applications in the environmental and earth sciences.

Acknowledgements

This research was supported by Research and Equipment Grants from the Natural Sciences and Engineering Research Council of Canada (NSERC), Alberta Research Excellence and IIPP Grants, University of Lethbridge Faculty Research and ULRF Grants, and a Fulbright Senior Scholarship awarded to Dr. Peddle. We also acknowledge funding through NSERC grants to Dr. Miller and Dr. LeDrew, and support from the University of Waterloo, York University, and CRESTech.

Appendix A. Equations used in the computation of solar zenith angle (SZA) and solar azimuth angle (Az_{Θ}), given date, time, latitude and longitude. Terms defined in text

$$\mathrm{Tu}_1 = (\mathrm{JD} - 2451545) + (1.002738\ \mathrm{TM}), \tag{A.1}$$

$$L_{\Theta} = 280.46 + 0.9856474\ \mathrm{Tu}_1, \tag{A.2}$$

$$g = 357.528 + 0.9856003\ \mathrm{Tu}_1, \tag{A.3}$$

$$L_{\mathrm{e}} = L_{\Theta} + 1.915\ \sin(g) + 0.02\ \sin(2g), \tag{A.4}$$

$$d_\Theta = 1.00014 - 0.01671\cos(g) - 0.00014\cos(2g), \quad (A.5)$$

$$\mathrm{oe} = 23.439 - 0.0000004\,\mathrm{Tu}_1, \quad (A.6)$$

$$\mathrm{RA}_\Theta = a\tan(\cos(\mathrm{oe})\tan(L_e))/15, \quad (A.7)$$

$$\mathrm{DEC}_\Theta = a\sin(\sin(\mathrm{oe})\sin(L_e)), \quad (A.8)$$

$$\mathrm{DEC}_z = \mathrm{Latitude}, \quad (A.9)$$

$$\mathrm{Tu}_2 = (\mathrm{JD} - 2451545)/36525, \quad (A.10)$$

$$\mathrm{GMST} = (24110.54841 + 8640184.812866\,\mathrm{Tu}_2 + 0.093104\,\mathrm{Tu}_2^2 - 0.0000062\,\mathrm{Tu}_2^3)/3600 + 1.002738\,\mathrm{TM}\ 24, \quad (A.11)$$

$$\mathrm{Ra}_z = \mathrm{LMST} = \mathrm{GMST} + (\mathrm{Longitude}/15), \quad (A.12)$$

$$\mathrm{SZA} = Z_\Theta = a\cos(\sin(\mathrm{DEC}_z)\sin(\mathrm{DEC}_\Theta) + \cos(\mathrm{DEC}_z)\cos(\mathrm{DEC}_\Theta)\cos((\mathrm{RA}_z - \mathrm{RA}_\Theta)\,15)), \quad (A.13)$$

$$\mathrm{Az}_\Theta = a\sin(\sin((\mathrm{RA}_z - \mathrm{RA}_\Theta)\,15) \times \cos(\mathrm{DEC}_\Theta)/\sin(Z_\Theta)). \quad (A.14)$$

Notes: L_Θ, g, and L_e must be scaled to 0–360°; LMST must be scaled to 0–24 h.

d_Θ is in astronomical units (AU), where $1\,\mathrm{AU} = 1.495985 \times 10^8$ km.

RA and DEC are equivalent to latitude and longitude on earth, and are fixed with the motion of the stars, not with the rotation of the earth. RA expressed as time (0–24 h), not degrees.

References

Adams, J.B., Smith, M.O., Gillespie, A.R., 1993. Imaging spectroscopy: interpretation based on spectral mixture analysis. In: Pieters, C.M., Englert, P.A.J. (Eds.), Topics in Remote Sensing IV: Remote Geochemical Analysis: Elemental and Mineralogical Composition. Cambridge University Press, Cambridge, pp. 145–166.

ASD, 1993. Personal Spectroradiometer II Reference Manual. Analytical Spectral Devices Inc., Boulder, CO.

ASD, 1998. FieldSpec FR User's Guide. Analytical Spectral Devices Inc., Boulder, CO, 47pp.

Bishop, R.L. (Ed.), 1994. Observers Handbook. Royal Astronomical Society of Canada, University of Toronto Press, Toronto, Canada, 142pp.

Blackburn, G.A., Milton, E.J., 1995. Ecology through spectrometry: the detection and classification of canopy gaps in deciduous woodlands. In: Mather, P.M. (Ed.), Understanding the Terrestrial Environment: Remote Sensing Data Systems and Networks. Wiley, Chichester, pp. 175–187.

Curran, P.J., 1985. Principles of Remote Sensing. Longmans, London, 282pp.

Deering, D.W., 1989. Field measurements of bi-directional reflectance. In: Asrar, G. (Ed.), Theory and Applications of Optical Remote Sensing. Wiley, New York, pp. 14–65.

Duffett-Smith, P., 1990. Practical Astronomy. Cambridge University Press, Cambridge, 421pp.

Eastman Kodak, 1983. Instructions for use of the Kodak neutral test card. Publication 092-4-80-ABX. Eastman Kodak Company, Rochester, New York, 7pp.

Franklin, J., 1995. Predictive vegetative mapping: geographic modeling of biospatial patterns in relation to environmental gradients. Progress in Physical Geography 19 (4), 474–499.

Franklin, J., Prince, S.D., Strahler, A.H., Hanan, N.P., Simonett, D.S., 1991. Reflectance and transmittance properties of West Africa savanna trees from ground radiometer measurements. International Journal of Remote Sensing 12 (6), 1369–1385.

Goward, S.N., Huemmrich, K.F., Waring, R.H., 1994. Visible-near infrared spectral reflectance of landscape components in western Oregon. Remote Sensing of Environment 47, 190–203.

Gray, L., Freemantle, J., Shepherd, P., Miller, J.R., Harron, J., Hersom, C., 1997. Characterization and calibration of the CASI airborne imaging spectrometer for BOREAS. Canadian Journal of Remote Sensing (Special Issue: BOREAS) 23 (2), 188–195.

Hall, F.G., Knapp, D.E., Huemmrich, K.F., 1997. Physically based classification and satellite mapping of biophysical characteristics in the southern boreal forest. Journal of Geophysical Research (BOREAS Special Issue) 102 (D24), 29,567–29,580.

Hall, F.G., Shimabukuro, Y.E., Huemmrich, K.F., 1995. Remote sensing of forest biophysical structure in boreal stands of *Picea mariana* using mixture decomposition and geometric reflectance models. Ecological Applications 5 (4), 993–1013.

Halliwell, D., Apps, M.J., 1996. BOREAS biometry and auxiliary sites: overstorey and understorey data. Technical Report, Northern Forestry Centre, Canadian Forest Service — Northwest Region. Edmonton, AB, Version 2.0, 256pp.

Hanan, N.P., Prince, S.D., Franklin, J., 1993. Reflectance properties of West Africa savanna trees from ground radiometer measurements. II. Classification of components. International Journal of Remote Sensing 14 (6), 1081–1097.

Hsia, J.J., Weidner, V.R., 1981. NBS 45°/normal reflectometer for absolute reflectance factors. Metrologia 17, 97–102.

Jackson, R.D., Clarke, T.R., Moran, M.S., 1992. Bidirectional calibration results for 11 Spectralon and 16 BaSO4 reference reflectance panels. Remote Sensing of Environment 40, 2310–2319.

Johnson, R.L., Peddle, D.R., Hall, R.J., Mah, S., 1999. Spectral mixture analysis of montane forest biophysical parameters: a comparison of endmembers from airborne imagery and a field spectroradiometer. Proceedings of the Fourth International Airborne Remote Sensing Conference and 21st

Canadian Symposium on Remote Sensing, Ottawa, Canada, Vol. II, pp. 107–114.

Labsphere, 1998. Reflectance characteristics of Spectralon panels. Reflectance Calibration Laboratory. Labsphere Inc., Sutton, NH, USA, 9pp.

Li, X., Strahler, A.H., 1992. Geometric-optical bidirectional reflectance modeling of the discrete crown vegetation canopy: effect of crown shape and mutual shadowing. IEEE Transactions on Geoscience and Remote Sensing 30 (2), 276–292.

Microsoft, 1997. Excel User's Guide, Excel version 5. 0. Microsoft Office. Microsoft Corporation, USA, 536pp.

Middleton, E.M., Chan, S.S., Ruskin, R.J., Mitchell, S.K., 1997. Optical properties of black spruce and jack pine needles at BOREAS sites in Saskatchewan, Canada. Canadian Journal of Remote Sensing (Special Issue: BOREAS) 23 (2), 108–119.

Miller, J., White, P., Chen, J., Peddle, D., McDermid, G., Fournier, R., Shepherd, P., Rubinstein, I., Freemantle, J., Soffer, R., LeDrew, E., 1997. Seasonal change in understorey reflectance of boreal forests and influence on canopy vegetation indices. Journal of Geophysical Research (BOREAS Special Issue) 102 (D24), 29,475–29,482.

Milton, E.J., 1987. Principles of field spectroscopy. International Journal of Remote Sensing 8, 1807–1827.

Milton, E.J., 1989. On the suitability of Kodak neutral test cards as reflectance standards. International Journal of Remote Sensing 10, 1041–1047.

Milton, E.J., Goetz, A.F.H., 1997. Atmospheric influences on field spectrometry: observed relationships between spectral irradiance and the variance in spectral reflectance. In: Guyot, G., Phulpin, T. (Eds.), Seventh International Symposium on Physical Measurements and Signatures in Remote Sensing, Vol. 1. Balkema, Rotterdam, pp. 109–114.

Milton, E.J., Rollin, E.M., Emery, D.R., 1995. Advances in field spectroscopy. In: Danson, F.M., Plummer, S.E. (Eds.), Advances in Environmental Remote Sensing. Wiley, Chichester, pp. 9–32.

Misurak, K.M., Barber, D.G., LeDrew, E.F., 1993. Seasonal sea ice monitoring and modeling site: SIMMS 1993 data report. Waterloo Laboratory for Earth Observations, Department of Geography, University of Waterloo, Waterloo, ON, Canada. ISTS-EOL-SIMS Report No. TR93-007, 377pp.

Nelson, B., Kapos, V., Adams, J., Oliveira, W., Braun, O., Amaral, I., 1994. Forest disturbance by large blowdowns in the Brazilian Amazon. Ecology 75 (3), 853–858.

O'Neil, N.T., Zagolski, F., Bergeron, M., Royer, A., Miller, J.R., Freemantle, J., 1997. Atmospheric correction validation of CASI images acquired over the BOREAS Southern Study Area. Canadian Journal of Remote Sensing (Special Issue: BOREAS) 23 (2), 143–162.

Palmer, J.M., 1982. Field standards of reflectance. Photogrammetric Engineering & Remote Sensing 48, 1623–1625.

Peddle, D.R., 1998. Field spectroradiometer data acquisition and processing for spectral mixture analysis in forestry and agriculture. Proceedings of the First International Conference on Geospatial Information in Agriculture and Forestry, Vol. 2, Lake Buena Vista, FL, USA, pp. 645–652.

Peddle, D.R., Hall, F.G., LeDrew, E.F., 1999b. Spectral mixture analysis and geometric optical reflectance modeling of boreal forest biophysical structure. Remote Sensing of Environment 67 (3), 288–297.

Peddle, D.R., Hall, F.G., LeDrew, E.F., Knapp, D.E., 1997. Classification of forest land cover in BOREAS. II: Comparison of results from a sub-pixel scale physical modeling approach and a training based method. Canadian Journal of Remote Sensing (Special Issue: BOREAS) 23 (2), 131–142.

Peddle, D.R., Johnson, R.L., 2000. Spectral mixture analysis of airborne remote sensing imagery for improved prediction of leaf area index in mountainous terrain, Kananaskis Alberta. Canadian Journal of Remote Sensing 26 (3), 176–187.

Peddle, D.R., LeDrew, E.F., Holden, H.M., 1995. Spectral mixture analysis of coral reef abundance from satellite imagery and in situ ocean spectra, Savusavu Bay, Fiji. Third Thematic Conference on Remote Sensing of Marine and Coastal Environments, Vol. II, Seattle, WA, USA, pp. 563–575.

Peddle, D.R., Smith, A.M., Ivie, C., Bullock, M., Russell, S., 1999a. Spectral mixture analysis of agricultural crops under different irrigation regimes: scene fraction validation in potato plots. Proceedings of the Fourth International Airborne Remote Sensing Conference and 21st Canadian Symposium on Remote Sensing, Vol. II, Ottawa, Canada, pp. 275–282.

Philipson, W.R., Gordon, D.K., Philpot, W.D., Duggin, M.J., 1989. Field reflectance calibration with grey standard reflectors. International Journal of Remote Sensing 10, 1035–1039.

Roberts, D.A., Smith, M.O., Adams, J.B., 1993. Green vegetation, nonphotosynthetic vegetation and soils in AVIRIS data. Remote Sensing of Environment 44, 255–269.

Rollin, E.M., Milton, E.J., Emery, D.R., 2000. Reflectance panel anisotropy and diffuse radiation — some implications for field spectroscopy. International Journal of Remote Sensing 21 (15), 2799–2810.

Rosema, A., Verhoef, W., Noorbergen, H., Borgesius, J., 1992. A new light interaction model in support of forest monitoring. Remote Sensing of Environment 42, 23–41.

Sellers, P., Hall, F., Margolis, H., Kelly, B., Baldocchi, D., den Hartog, J., Cihlar, J., Ryan, M., Goodison, B., Crill, P., Ranson, J., Lettenmaier, D., Wickland, D., 1995. The Boreal Ecosystem-Atmosphere Study (BOREAS): an overview and early results from the 1994 field year. Bulletin American Meteorological Society 76 (9), 1549–1577.

Sellers, P.J., Schimel, D., 1993. Remote sensing of the land biosphere and biogeochemistry in the EOS era: science priorities, methods and implementation. Global and Planetary Change 7, 279–297.

Soffer, R.J., Harron, J.W., Miller, J.R., 1995. Characterisation of Kodak grey cards as reflectance reference panels in support of BOREAS field activities. Proceedings of the 17th Canadian Symposium on Remote Sensing, Vol. I, Saskatoon, SK, Canada, pp. 357–362.

Strahler, A.H., Jupp, D.L.B., 1990. Geometric-optical modelling of forests as remotely sensed scenes composed of three-dimensional, discrete objects. In: Myneni, R., Ross, J. (Eds.), Photon-Vegetation Interactions: Applications in Optical Remote Sensing and Plant Ecology. Springer, Heidelberg, Germany, pp. 162–190.

Syrén, P., 1994. Reflectance anisotropy for nadir observations of coniferous forest canopies. Remote Sensing of Environment 49, 72–80.

Teillet, P.M., 1995. The role of surface observations in support of remote sensing. In: LeDrew, E.F., Strome, M., Hegyi, F. (Eds.), The Canadian Remote Sensing Contribution to Understanding Global Change. Department of Geography Publication Series, No. 38, University of Waterloo, Waterloo, ON, Canada, pp. 333–352.

Weidner, V.R., Hsia, J.J., 1981. Reflection properties of pressed polytetrafluoroethylene powder. Journal of the Optical Society of America 71 (7), 856–861.